



# Preparation of nanostructured $\text{Al}_2\text{O}_3$ – $\text{TiO}_2$ composite films by MOCVD

J.A. Galaviz Pérez<sup>a,\*</sup>, J. A. Montes de Oca Valero<sup>b</sup>, J.R. Vargas García<sup>a</sup>, H.J. Dorantes Rosales<sup>a</sup>

<sup>a</sup> Dept of Metallurgical Eng., National Polytechnic Institute, México 07300 DF, Mexico

<sup>b</sup> Research Center on Applied Science and Advanced Technology, Km 14.5 Tampico-Puerto industrial Altamira road, Altamira 89600, Tamaulipas, Mexico

## ARTICLE INFO

### Article history:

Received 9 July 2008

Received in revised form 20 October 2009

Accepted 23 October 2009

Available online 29 October 2009

### Keywords:

Nanostructures  
Alumina–titania  
Composite films  
MOCVD

## ABSTRACT

Nanostructured  $\text{Al}_2\text{O}_3$ – $\text{TiO}_2$  composite films were prepared on glass substrates by metalorganic chemical vapor deposition (MOCVD) using aluminum acetylacetonate and titanium tetraisopropoxide precursors. Oxygen and argon were used as the reactive and carrier gases, respectively. Deposition temperature ( $T_{\text{dep}}$ ) was varied from 723 to 873 K and total pressure was kept constant at 133–266 Pa. The formation of composite films was achieved by mixing the precursor vapors, which were obtained by heating the aluminum and titanium precursors at 403 and 323–353 K, respectively. The films were characterized by XRD, SEM, EPMA and TEM. The crystalline structure and the surface morphology of the nanostructured  $\text{Al}_2\text{O}_3$ – $\text{TiO}_2$  composite films were strongly dependent on the precursor and deposition temperatures.

© 2009 Elsevier B.V. All rights reserved.

## 1. Introduction

For long time,  $\text{Al}_2\text{O}_3$  and  $\text{TiO}_2$  have been highly recognized for their effectiveness in a wide variety of practical applications. As a consequence, many efforts have been undertaken to combine their extraordinary properties such as in  $\text{Al}_2\text{O}_3$ – $\text{TiO}_2$  composite coatings [1–3],  $\text{Al}_2\text{O}_3$ – $\text{TiO}_2$  composite powders [4–5] or  $\text{TiO}_2$  deposition on  $\text{Al}_2\text{O}_3$  [6–8]. In recent years, additional efforts have been devoted to the synthesis of  $\text{Al}_2\text{O}_3$ – $\text{TiO}_2$  nanocomposite architectures. Thus, various synthesis methods have been employed to attempt well-dispersed nanostructured composites. Plasma spraying has been the most common preparation method to attain thick-enough  $\text{Al}_2\text{O}_3$ – $\text{TiO}_2$  composite coatings, which have been improved by supplying the individual components in nanometric sizes [9–10]. The deposition of  $\text{TiO}_2$  on nanosized powders of  $\text{Al}_2\text{O}_3$  or alternatively, the formation of  $\text{Al}_2\text{O}_3$ – $\text{TiO}_2$  nanocomposite powders have been investigated by the sol–gel method over the last decade [11–12]. The synthesis of  $\text{Al}_2\text{O}_3$ – $\text{TiO}_2$  composite films by using the chemical vapor deposition (CVD) method has been more recent [13–14]. So far, the CVD  $\text{Al}_2\text{O}_3$ – $\text{TiO}_2$  composite films have been prepared by using traditional Al and Ti chloride precursors and the resulting films have been amorphous in nature [14]. Here, we report the preparation of nanostructured  $\text{Al}_2\text{O}_3$ – $\text{TiO}_2$  composite films by CVD using metalorganic precursors (MOCVD) that allow deposition temperatures as low as 723 K. The nanostructured composite films consist of crystalline  $\text{TiO}_2$  in an amorphous  $\text{Al}_2\text{O}_3$  matrix.

## 2. Experimental

The nanostructured  $\text{Al}_2\text{O}_3$ – $\text{TiO}_2$  composite films were prepared on amorphous glass slides (25 mm × 30 mm × 1 mm) in a horizontal hot-wall MOCVD type reactor, which is depicted in Fig. 1. Titanium tetraisopropoxide,  $\text{Ti}[\text{OCH}(\text{CH}_3)_2]_4$  (abbr. TTIP) and aluminum acetylacetonate,  $\text{Al}(\text{CH}_3-\text{COCHCO}-\text{CH}_3)_3$  (abbr.  $\text{Al}(\text{acac})_3$ ) were used as precursors. The MOCVD apparatus consists of: (1) quartz tube reactor, (2) electrical furnace, (3) substrate, (4) TTIP precursor, (5)  $\text{Al}(\text{acac})_3$  precursor, (6)  $\text{Al}(\text{acac})_3$  thermocouple, (7) substrate thermocouple, (8) thermal bath, and (9) vacuum pump. The liquid TTIP precursor was evaporated in a thermal bath at 323–353 K ( $T_{\text{prec}}^{\text{Ti}}$ ) and carried by  $\text{O}_2$  gas ( $FR_{\text{O}_2} = 25$  sccm) into the tube reactor, while the powdered  $\text{Al}(\text{acac})_3$  precursor was evaporated inside the reactor at 403 K. Both precursor vapors were mixed with Ar ( $FR_{\text{Ar}} = 25$  sccm) and then carried to the deposition zone. The deposition temperature ( $T_{\text{dep}}$ ) was varied from 723 to 873 K and the total pressure ( $P_{\text{tot}}$ ) was controlled at 133–266 Pa. The crystal structure and morphology of the composite films were investigated by X-ray diffraction (XRD) using  $\text{Cu K}\alpha$  radiation, scanning (SEM) and transmission (TEM) electron microscopies, respectively. Chemical composition of the films was analyzed by electron-probe microanalysis (EPMA).

## 3. Results and discussion

Fig. 2 shows the effect of deposition temperature on the XRD patterns of  $\text{Al}_2\text{O}_3$ – $\text{TiO}_2$  composite films prepared at  $P_{\text{tot}} = 133$ –266 Pa,  $T_{\text{prec}}^{\text{Ti}} = 323$  K and  $T_{\text{prec}}^{\text{Al}} = 403$  K on amorphous glass substrates. No observable XRD reflections were obtained at  $T_{\text{dep}} = 723$  K suggesting the formation of a significant amorphous film, thick enough to hide the amorphous signal from the substrate. Previous results have shown that crystalline  $\text{TiO}_2$  films can be obtained by CVD at temperatures as low as 623 K using the TTIP precursor [15]. In addition, the simultaneous growth of amorphous alumina and crystalline titania has been reported by using the sol–gel method [16]. Therefore, the present results may imply the formation of films consisting of amorphous alumina in coexistence with crystalline titania. As

\* Corresponding author.

E-mail address: [jgalaviz@ipn.mx](mailto:jgalaviz@ipn.mx) (J.A.G. Pérez).

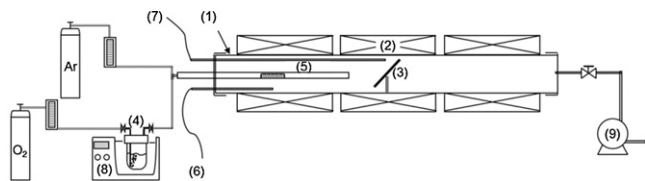


Fig. 1. Schematic representation of the MOCVD apparatus.

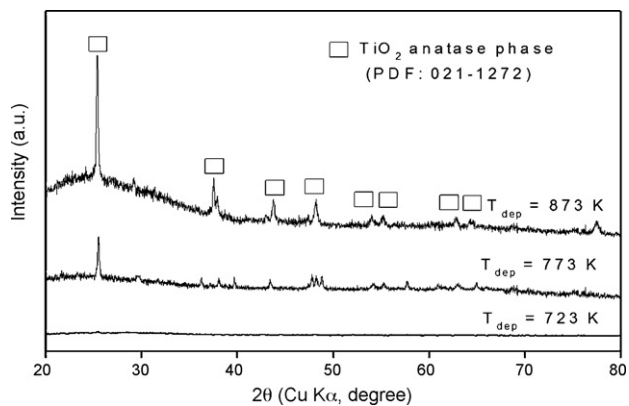


Fig. 2. Effect of the deposition temperature on the XRD patterns of  $\text{Al}_2\text{O}_3$ - $\text{TiO}_2$  composite films.

deposition temperature increases, the crystalline nature of films is more evident. At  $T_{\text{dep}} = 873$  K, most of the reflections correspond to those of the  $\text{TiO}_2$  anatase phase, while at  $T_{\text{dep}} = 773$  K only a few of them are present. This suggests that the films obtained at  $T_{\text{dep}} = 873$  K mainly consist of anatase phase and amorphous alumina, most likely. In fact, the semi-quantitative EPMA analysis indicated an Al/O ratio consistent with that of the  $\text{Al}_2\text{O}_3$  stoichio-

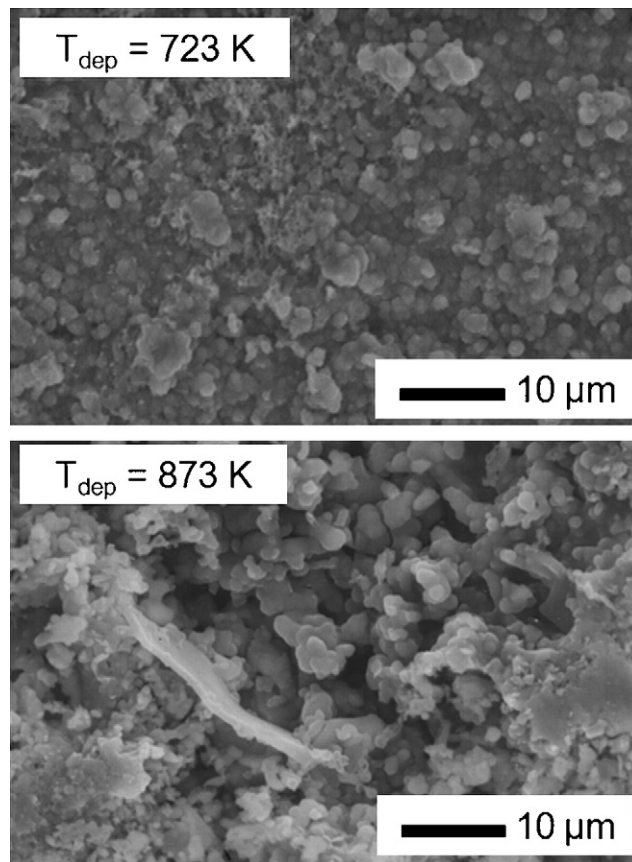


Fig. 3. Influence of the deposition temperature ( $T_{\text{dep}}$ ) on the film surface morphology.

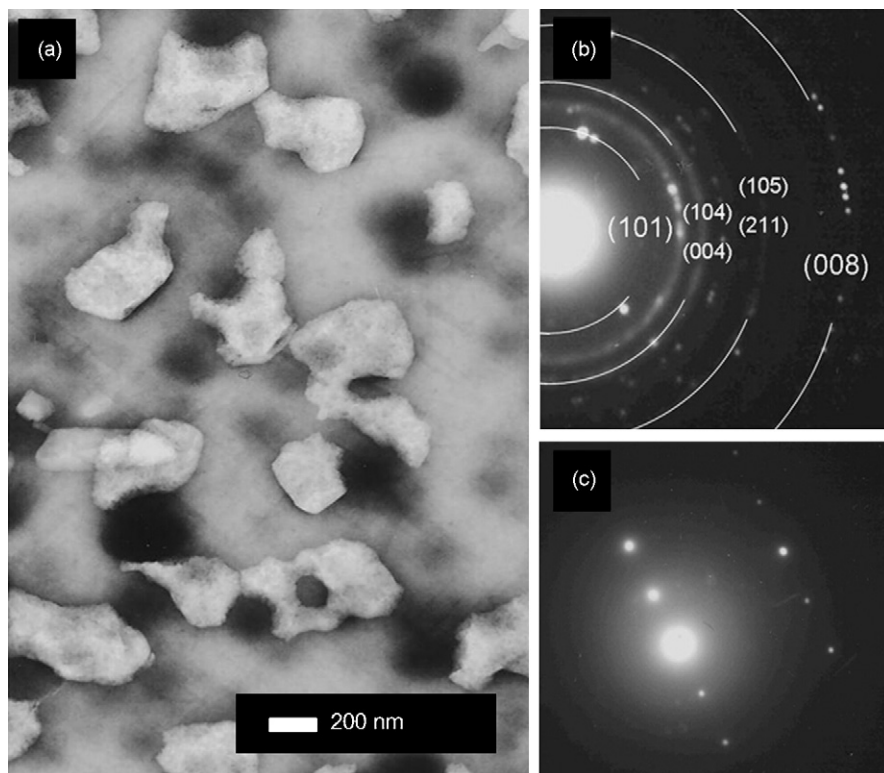


Fig. 4. Bright field TEM image and SAED patterns of the composite films prepared at  $T_{\text{dep}} = 773$  K,  $T_{\text{prec}}^{\text{Ti}} = 323$  K and  $T_{\text{prec}}^{\text{Al}} = 403$  K.

metric ratio. In contrast, films prepared at  $T_{\text{dep}} = 773$  K may consist of various crystalline Ti–O phases (e.g.  $\text{TiO}$ ,  $\text{Ti}_4\text{O}_{10}$  and  $\text{Ti}_7\text{O}_{13}$ ) which are not necessarily  $\text{TiO}_2$  anatase or rutile.

Fig. 3 illustrates the influence of the deposition temperature ( $T_{\text{dep}}$ ) on the film surface morphology. At  $T_{\text{dep}} = 723$  K, the films exhibit a rough surface resulting from agglomerated particles ( $\sim 1 \mu\text{m}$  in size) probably consisting of smaller primary particles, which may cause the broad reflections in Fig. 2. As the deposition temperature increases ( $T_{\text{dep}} = 873$  K), the composite films show rougher surfaces characterized by a more open porous morphology. This increase in surface area could be the result of higher deposition rates promoted by the raise in precursor vapor concentrations. The kinetic studies on the formation of  $\text{TiO}_2$  and  $\text{Al}_2\text{O}_3$  films using the individual precursors TTIP or  $\text{Al}(\text{acac})_3$ , respectively report a surface reaction regime controlling the growth of the films in the deposition temperature range of 523–873 K [18–19]. As the  $\text{Al}_2\text{O}_3$ – $\text{TiO}_2$  composite films were prepared at  $T_{\text{dep}} = 723$ –873 K, a considerable increment in the deposition rate for this temperature range could be expected. On the other hand, it was observed that  $\text{Al}_2\text{O}_3$ – $\text{TiO}_2$  composite films showed notable rough surface morphologies at  $T_{\text{prec}}^{\text{Ti}} = 333$ –363 K. These results are consistent with those previously reported for the deposition of titania using the TTIP precursor under similar deposition conditions [17].

A typical bright field TEM image of the composite films prepared at  $T_{\text{dep}} = 773$  K,  $T_{\text{prec}}^{\text{Ti}} = 323$  K and  $T_{\text{prec}}^{\text{Al}} = 403$  K is shown in Fig. 4a. This image reveals a homogeneous mixture of two phases. One is a continuous matrix (white areas) basically consisting of nanocrystalline  $\text{TiO}_2$  in anatase phase as suggested by the characteristic ring pattern of Fig. 4b. The EPMA analysis further suggests that  $\text{Al}_2\text{O}_3$  is also a component of this continuous matrix. This implies that the continuous matrix is essentially amorphous  $\text{Al}_2\text{O}_3$  with incorporated crystalline  $\text{TiO}_2$  anatase particles. Higher magnification observations indicated that the  $\text{TiO}_2$  anatase particles are about 20 nm in size. The second phase (dark areas) was attributed to crystalline Ti–O phases such as  $\text{TiO}$ ,  $\text{Ti}_4\text{O}_{10}$  or  $\text{Ti}_7\text{O}_{13}$ , which display the spot pattern of Fig. 4c.

#### 4. Conclusions

Nanostructured  $\text{Al}_2\text{O}_3$ – $\text{TiO}_2$  composite films were prepared by MOCVD. The composite films consist of a continuous matrix of

nanocrystalline  $\text{TiO}_2$  anatase particles ( $\sim 20$  nm in size) embedded in amorphous  $\text{Al}_2\text{O}_3$  and crystalline areas of Ti–O phases different from anatase or rutile. The crystalline structure and the surface morphology of the nanostructured  $\text{Al}_2\text{O}_3$ – $\text{TiO}_2$  composite films were strongly dependent on the precursor and deposition temperatures.

#### Acknowledgments

Authors wish to thank the financial support through the projects IPN-SIP-2007-0618, IPN-SIP-2008-0801 and IPN-SIP 20080927. Author J. A. Galaviz Pérez wishes to thank the National Council of Science and Technology (CONACYT) for the financial support for obtaining the master degree.

#### References

- [1] H. Choi, E. Stathatos, D. Dionysiou, *Desalination* 202 (2007) 199–206.
- [2] J. Grzechowiak, I. Wereszczako-Zlielinzka, K. Mrozinska, *Catal. Today* 119 (2007) 23–30.
- [3] T. Hejwowski, A. Weroni, *Vacuum* 65 (2002) 427–432.
- [4] J. Mani, S. Ananthakumar, P. Mukundan, K. Gopakumar, *J. Am. Ceram. Soc.* 90 (10) (2007) 3091–3094.
- [5] A.L. Ahmad, M.R. Othman, N.F. Idrus, *J. Am. Ceram. Soc.* 89 (10) (2006) 3187–3193.
- [6] H. Choi, E. Stathatos, D.D. Dionysiou, *Appl. Catal. B Environ* 63 (2006) 60–67.
- [7] G. Carta, G. Rosetto, P. Zanella, S. Battaini, S. Sitran, P. Guerriero, G. Cavinato, L. Armelao, E. Tondello, *Surf. Coat. Technol.* 160 (2002) 124–131.
- [8] Z. Ding, X. Hu, P.L. Yue, P.F. Greenfield, *Catal. Today* 68 (2001) 173–182.
- [9] M. Gopalakrishnan, R. Krishnamurthy, C.V. Gokulathnam, *J. Mater. Process. Technol.* 185 (2007) 233–237.
- [10] P. Bansal, N.T. Padture, A. Vasiliev, *Acta Mater.* 51 (2003) 2959–2970.
- [11] T. Hernandez, M.C. Bautista, *J. Eur. Ceram. Soc.* 25 (2005) 663–672.
- [12] A.A. Cecilio, S.H. Pulcinelli, C.V. Santilli, Y. Maniette, *J. Sol–Gel Sci. Technol.* 31 (2004) 87–93.
- [13] B.-H. Kim, J.-Y. Lee, J.-H. Choa, M. Higuchi, N. Mizutani, *Mater. Sci. Eng. B* 107 (2004) 289–294.
- [14] D.-H. Kuo, C.-N. Shueh, *J. Non-Cryst. Solids* 336 (2004) 120–127.
- [15] K.-H. Ahn, Y.-B. Park, D.-H. Park, *Surf. Coat. Technol.* 171 (2003) 198–204.
- [16] E. Otterstein, G. Karapetyan, R. Nicula, M. Stir, C. Schick, E. Burkel, *Thermochim. Acta* 468 (2008) 10–14.
- [17] M.I.B. Bernardi, E.J.H. Lee, P.N. Lisboa-Filho, E.R. Leite, E. Longo, A.G. Souza, *Cerâmica* 308 (2002) 192–198.
- [18] K. Nakaso, K. Okuyama, M. Shimada, S.E. Prastinis, *Chem. Eng. Sci.* 58 (2003) 3327–3335.
- [19] T. Maruyama, S. Arai, *Appl. Phys. Lett.* 60 (3) (1992) 322–324.